ACI JOURNAL TECHNICAL PAPER

Title no. 83-22

The Modified Compression-Field Theory for Reinforced Concrete Elements Subjected to Shear

by Frank J. Vecchio and Michael P. Collins

An analytical model is presented that is capable of predicting the load-deformation response of reinforced concrete elements subjected to in-plane shear and normal stresses. In the model, cracked concrete is treated as a new material with its own stress-strain characteristics. Equilibrium, compatibility, and stress-strain relationships are formulated in terms of average stresses and average strains. Consideration is also given to local stress conditions at crack locations.

*The stress-strain relationships for the cracked concrete were determined by testing 30 reinforced concrete panels under a variety of well-defined uniform biaxial stresses including pure shear. It was found that cracked concrete subjected to high tensile strains in the direction normal to the compression is softer and weaker in compression than concrete in a standard cylinder test. **Additionally,** significant tensile stresses were found in the concrete between the cracks even at very high values of average tensile strain.*

Keywords: aggregate interlock; axial loads; **biaxial loads; cracking (fracturing);** crack width and spacing; finite element method; **offshore** structures; **reinforced concrete; shear strength;** stiffness; **stresses; stress-strain relationships;** structural analysis; tension; **tests.**

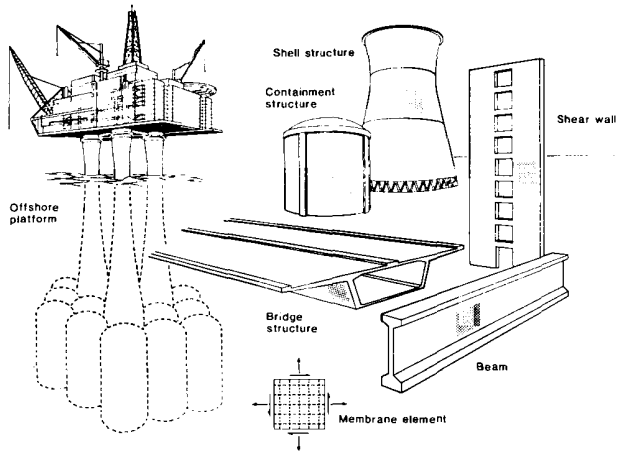

Fig. 1 — Structures idealized as an assemblage of membrane elements

The safety of large-scale, complex civil engineering structures such as offshore oil platforms, containment structures for nuclear power plants, high-rise buildings, and long-span bridges depends on the designer's ability to predict how such structures will respond under extreme environmental and man-made hazards. In making this prediction, the designer typically conceptualizes the actual structure as an assemblage of simpler elements. Predicting the structural response then involves the two interrelated tasks of determining how the load is shared among the elements of the structure (global analysis) and how each element responds to its applied loads (element analysis).

During the last 25 years, techniques have been developed for global analysis which are truly impressive in their power and elegance.[1-3] Unfortunately, the models available for reinforced concrete element analysis[4-7] match neither the sophistication of the global structural analysis procedures nor the computational power now available to the structural engineer.

This paper will focus on the response of rectangular reinforced concrete elements subjected to in-plane shear and axial stresses (i.e., membrane stresses). Such a membrane element may be used in modeling the response of such structures as those shown in Fig. 1, where the load is primarily carried through the action of in-plane stresses.

Predicting the response of the simple reinforced concrete element shown in Fig. 1 is not as straightforward a task as it would first appear. Under a particular set of loads, new cracks may form, pre-existing cracks may propagate or close, and the forces will be resisted by a structural system consisting of concrete bodies joined by reinforcing bars. The stresses in the reinforcing bars will vary along the lengths of the bars, and will be highest at the crack locations. The concrete bodies will

Received July 29, 1985, and reviewed under Institute publication policies.
 Pertinent discussion will be published in the January-February 1987 ACI JOURNAL if received by Oct. 1, 1986.

ACI member Frank J. Vecchio is an assistant professor in the Department of Civil Engineering at the University of Toronto. Prior to joining the university he was a structural research engineer with Ontario Hydro, where he was involved in research related to the analysis and design of reinforced concrete nuclear power plant structures. He is a member of ACI Committee 435, Deflections of Structures.

Michael P. Collins, FACI, is a professor in the Department of Civil Engineering at the University of Toronto. He is chairman of Joint ACI-ASCE Committee 445, Shear and Torsion; chairman of the Canadian Standards Association (CSA) Technical Committee S 474, Concrete Offshore Structures; a Canadian delegate to Comité Euro-International du Béton; a member of CSA Technical Committee A23.3, Reinforced Concrete Design; and a member of ACI Committee 358, Concrete Guideways, and E901, Scholarships; and of Subcommittee 318E, Shear and Torsion. He has acted as a consultant on the shear design of Condeep concrete offshore platforms.

be bounded by rough crack surfaces capable of transmitting shear and compression at the contact locations, but not capable of transmitting tension. However, tensile stresses will exist in the concrete lying between the cracks. To date, there is no accepted theory capable of predicting the full load-deformation response of such an element. This was made evident in a recent international competition[8] in which 43 leading researchers from 13 different countries attempted to predict the load-deformation response of 4 of the reinforced concrete panels which were tested in this investigation. For one of the elements (PV25 in Table 1), the ratio of the highest to lowest prediction of strength was six to one. Not even the best entry was capable of predicting strengths to within 15 percent for each of the four panels. It should be emphasized that in choosing the four elements for the competition, elements whose behavior would be difficult to predict were deliberately chosen; thus, in none of the elements was the load capacity governed by overall yielding of the reinforcement. The predictions were strongly dependent on the assumed stress-strain characteristics of the concrete. While such heavily reinforced elements subjected to high shear are unusual in typical buildings, they often occur in offshore platforms and nuclear containment structures.

The modified compression-field theory presented here has been developed from the compression-field theory[9,10] for reinforced concrete in torsion and shear. In both models, the cracked concrete is treated as a new material with its own stress-strain characteristics. Equilibrium, compatibility, and stress-strain relationships are formulated in terms of average stresses and average strains. While the original compression-field theory ignored tension in the cracked concrete, this model takes into account tensile stresses in the concrete between the cracks, and employs experimentally verified average stress-average strain relationships for the cracked concrete.

DEFINITION OF THE PROBLEM

The membrane element shown in Fig. 2 represents a portion of a reinforced concrete structure. It is taken to be of uniform thickness and relatively small size, and

Table 1 — Summary of experimental program

Panel	Loading ratios $v:f_1:f_2$	Longitudinal steel ρ_1	Longitudinal steel f_{y1}, MPa	Transverse steel ρ_2	Transverse steel f_{y2}, MPa	Concrete ϵ'_c	Concrete f'_c, MPa	Experimental observations v_{u1}, MPa	Experimental observations v_u, MPa	Failure strains ϵ_1/ϵ_{y1}	Failure strains ϵ_2/ϵ_{y2}	Failure strains ϵ_2/ϵ'_c	Comments
PV1	1:0:0	0.0179	483	0.0168	483	−0.0022	−34.5	2.21	>8.02	0.91	1.04	0.48	Edge failure
PV2	1:0:0	0.0018	428	0.0018	428	−0.0023	−23.5	1.10	1.16	0.38	0.43	0.10	Precracked — warped
PV3	1:0:0	0.0048	662	0.0048	662	−0.0023	−26.6	1.66	3.07	0.67	0.73	0.21	Steel brittle fracture
PV4	1:0:0	0.0106	242	0.0106	242	−0.0025	−26.6	1.79	2.89	4.91	5.47	0.18	
PV5	1:0:0	0.0074	621	0.0074	621	−0.0025	−28.3	1.73	>4.24	0.80	0.83	0.30	Edge failure
PV6	1:0:0	0.0179	266	0.0179	266	−0.0025	−29.8	2.00	4.55	5.36	5.48	0.23	
PV7	1:0:0	0.0179	453	0.0179	453	−0.0025	−31.0	1.93	>6.81	0.84	0.85	0.35	Edge failure
PV8	1:0:0	0.0262	462	0.0262	462	−0.0025	−29.8	1.73	>6.67	0.56	0.59	0.38	Edge failure
PV9	1:0:0	0.0179	455	0.0179	455	−0.0028	−11.6	1.38	>3.74	0.59	0.47	1.05	Poorly cast — voids
PV10	1:0:0	0.0179	276	0.0100	276	−0.0027	−14.5	1.86	3.97	0.64	4.47	1.48	
PV11	1:0:0	0.0179	235	0.0131	235	−0.0026	−15.6	1.66	3.56	1.28	2.37	0.61	
PV12	1:0:0	0.0179	469	0.0045	269	−0.0025	−16.0	1.73	3.13	0.40	4.34	0.93	
PV13	1:0:0	0.0179	248	0	—	−0.0027	−18.2	1.73	2.01	0.61	8.56	0.37	
PV14	1:0:0	0.0179	455	0.0179	455	−0.0022	−20.4	1.93	>5.24	0.55	0.56	0.27	Edge failure
PV15	0:-1:0	0.0074	255	0.0074	255	−0.0020	−21.7	—	>(−19.6)'	−0.93	0.14	0.58	Loading stopped
PV16	1:0:0	0.0074	255	0.0074	255	−0.0020	−21.7	2.07	2.14	4.12	4.33	0.16	
PV17	0:-1:0	0.0074	255	0.0074	255	−0.0020	−18.6	—	(−21.3)'	−1.97	0.48	1.26	Explosive failure
PV18	1:0:0	0.0179	431	0.0032	412	−0.0022	−19.5	2.00	>3.04	0.46	3.36	0.36	Edge failure
PV19	1:0:0	0.0179	458	0.0071	299	**−0.0022**	−19.0	2.07	3.95	0.50	5.77	0.72	
PV20	1:0:0	0.0179	460	0.0089	297	**−0.0018**	−19.6	2.21	4.26	0.52	5.75	1.06	
PV21	1:0:0	0.0179	458	0.0130	302	−0.0018	−19.5	2.35	5.03	0.59	3.59	0.81	
PV22	1:0:0	0.0179	458	0.0152	420	−0.0020	−19.6	2.42	6.07	0.60	0.91	0.53	
PV23	1:-0.39:-0.39	0.0179	518	0.0179	518	−0.0020	−20.5	3.73	8.87	0.36	0.44	1.33	
PV24	1:-0.83:-0.83	0.0179	492	0.0179	492	**−0.0019**	−23.8	4.97	>7.94	−0.05	−0.03	0.37	Poorly cast — voids
PV25	1:-0.69:-0.69	0.0179	466	0.0179	466	−0.0018	−19.2	4.14	9.12	0.13	0.17	1.47	
PV26	1:0:0*	0.0179	456	0.0101	463	**−0.0019**	−21.3	2.00	5.41	0.58	1.16	0.53	
PV27	1:0:0	0.0179	442	0.0179	442	**−0.0019**	−20.5	2.04	6.35	0.52	0.53	0.59	
PV28	1:0.32:0.32	0.0179	483	0.0179	483	**−0.0019**	−19.0	1.66	5.80	0.92	0.85	1.28	
PV29	Changing	0.0179	441	0.0089	324	−0.0018	−21.7	2.21	5.87	0.38	1.80	0.71	
PV30	±1:0:0*	0.0179	437	0.0101	472	−0.0019	−19.1	1.55	>5.13	0.51	0.95	0.59	Edge failure

*Precracked in biaxial tension.
'Values of f_1.
Note: 1 MPa = 145 psi.

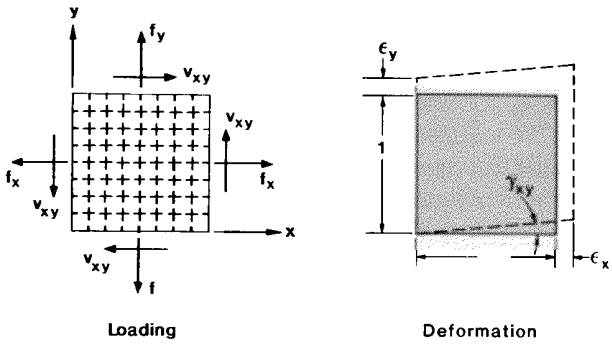

Fig. 2 — Membrane element

contains an orthogonal grid of reinforcement with the longitudinal (x) and transverse (y) axes chosen to coincide with the reinforcement directions. Loads acting on the element's edge planes are assumed to consist of the uniform axial stresses f_x and f_y and the uniform shear stress v_{xy}. Deformation of the element is assumed to occur such that the edges remain straight and parallel. The deformed shape is defined by the two normal strains ϵ_x and ϵ_y and the shear strain, γ_{xy}.

The problem at hand is to determine how the three in-plane stresses f_x, f_y, and v_{xy} are related to the three in-plane strains ϵ_x, ϵ_y, and γ_{xy}. In solving this problem, the following additional assumptions will be made:

1. For each strain state there exists only one corresponding stress state; situations in which the influence of loading history is significant will not be treated.
2. Stresses and strains can be considered in terms of average values when taken over areas or distances large enough to include several cracks.
3. The concrete and the reinforcing bars are perfectly bonded together at the boundaries of the element (i.e., no overall slip).
4. The longitudinal and transverse reinforcing bars are uniformly distributed over the element.

Tensile stresses and tensile strains will be treated as positive quantities while compressive stresses and strains will be taken as negative.

COMPATIBILITY CONDITIONS

Having assumed that the reinforcement is anchored to the concrete, compatibility requires that any deformation experienced by the concrete must be matched by an identical deformation of the reinforcement. Any change in concrete strain will be accompanied by an equal change in steel strain.

Nonprestressed reinforcement has the same initial strain as the surrounding concrete. Hence

$$\epsilon_{sx} = \epsilon_{cx} = \epsilon_x \tag{1}$$

and

$$\epsilon_{sy} = \epsilon_{cy} = \epsilon_y \tag{2}$$

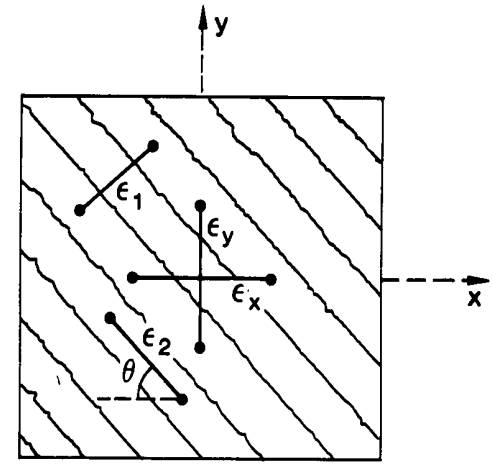

(a) Average Strains in Cracked Element

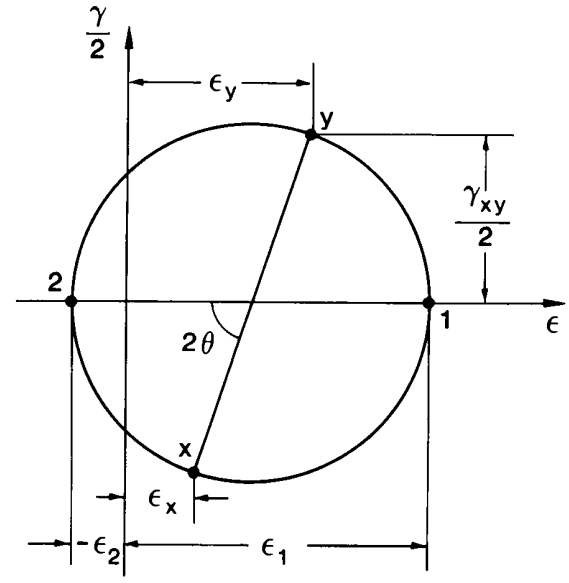

(b) Mohr's Circle for Average Strains

Fig. 3 — Compatibility conditions for cracked element

If the three strain components ϵ_x, ϵ_y, and γ_{xy} are known, then the strain in any other direction can be found from geometry. The Mohr's circle of strain shown in Fig. 3 elegantly summarizes the transformations involved. Useful relationships which can be derived from its geometry include

$$\gamma_{xy} = \frac{2\,(\epsilon_x - \epsilon_2)}{tan\theta} \tag{3}$$

$$\epsilon_x + \epsilon_y = \epsilon_1 + \epsilon_2 \tag{4}$$

and

$$tan^2\theta = \frac{\epsilon_x - \epsilon_2}{\epsilon_y - \epsilon_2} = \frac{\epsilon_1 - \epsilon_y}{\epsilon_1 - \epsilon_x} = \frac{\epsilon_1 - \epsilon_y}{\epsilon_y - \epsilon_2} = \frac{\epsilon_x - \epsilon_2}{\epsilon_1 - \epsilon_x} \tag{5}$$

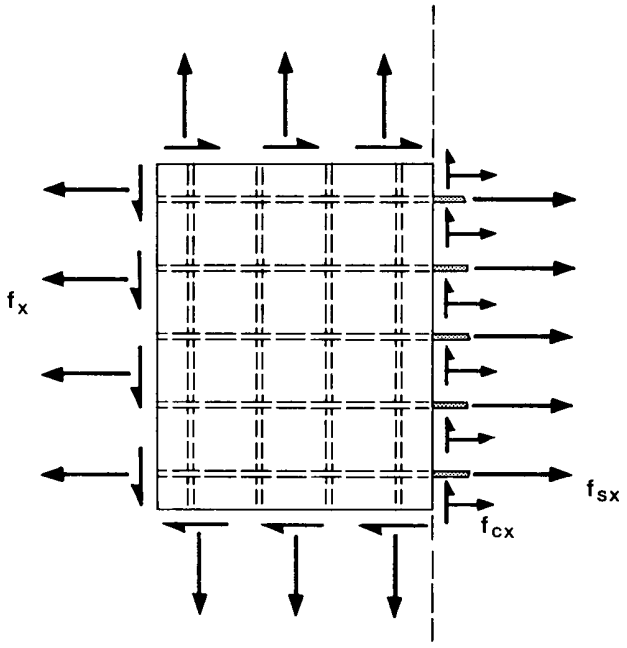

Fig. 4 — Free-body diagram of part of element

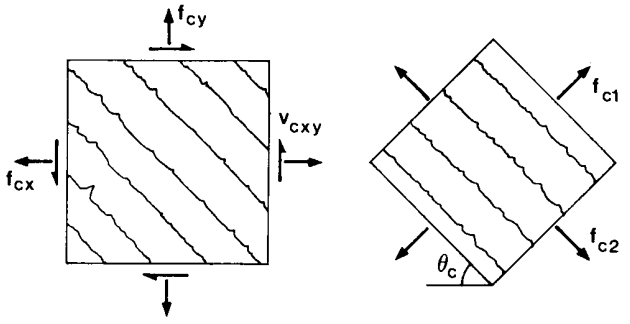

(a) Average Concrete Stresses

(b) Principal Stresses in Concrete

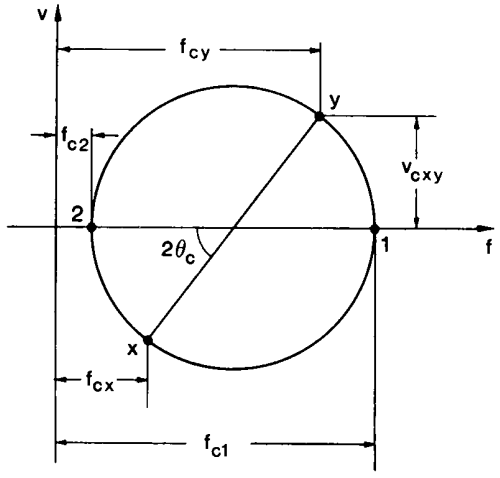

(c) Mohr's Circle for Average Concrete Stresses

Fig. 5 — Stresses in cracked concrete

where ϵ_1 is the principal tensile strain and ϵ_2 is the principal compressive strain.

EQUILIBRIUM CONDITIONS

The forces applied to the reinforced concrete element are resisted by stresses in the concrete and stresses in the reinforcement. For the free-body diagram shown in Fig. 4, the requirement that the forces sum to zero in the x-direction can be written as

$$\int_A f_x \, dA = \int_{A_c} f_{cx} \, dA_c + \int_{A_s} f_{sx} \, dA_s \tag{6}$$

Ignoring the small reduction in concrete cross-sectional area due to the presence of reinforcing bars, Eq. (6) becomes

$$f_x = f_{cx} + \rho_{sx} \cdot f_{sx} \tag{7}$$

In a similar fashion, the following equilibrium conditions can be derived

$$f_y = f_{cy} + \rho_{sy} \cdot f_{sy} \tag{8}$$

$$v_{xy} = v_{cx} + \rho_{sx} \cdot v_{sx} \tag{9}$$

and

$$v_{xy} = v_{cy} + \rho_{sy} \cdot v_{sy} \tag{10}$$

Assuming that

$$v_{cx} = v_{cy} = v_{cxy}$$

the stress conditions in the concrete are fully defined if f_{cx}, f_{cy}, and v_{cxy} are known.

The Mohr's circle for the concrete stresses shown in Fig. 5 yields the following useful relationships

$$f_{cx} = f_{c1} - v_{cxy}/tan\theta_c \tag{11}$$

$$f_{cy} = f_{c1} - v_{cxy} \cdot tan\theta_c \tag{12}$$

and

$$f_{c2} = f_{c1} - v_{cxy} \cdot (tan\theta_c + 1/tan\theta_c) \tag{13}$$

STRESS-STRAIN RELATIONSHIPS

Constitutive relationships are required to link average stresses to average strains for both the reinforcement and the concrete. These average stress-average strain relations may differ significantly from the usual local stress-local strain relations determined from standard material tests. Furthermore, the average stress-average strain relationships for the reinforcement and for the concrete will not be completely independent of each other, although this will be assumed to maintain the simplicity of the model.

The axial stress in the reinforcement will be assumed to depend on only one strain parameter, the axial strain in the reinforcement. It will be assumed further that the average shear stress on the plane normal to the reinforcement resisted by the reinforcement is zero. In relating axial stress to axial strain, the usual bilinear uniaxial stress-strain relationship shown in Fig. 6 will be adopted. Thus

$$f_{sx} = E_s \cdot \epsilon_x \leqslant f_{yx} \quad (14)$$

$$f_{sy} = E_s \cdot \epsilon_y \leqslant f_{yy} \quad (15)$$

$$v_{sx} = v_{sy} = 0 \quad (16)$$

In regard to the concrete, it will be assumed that the principal stress axes and principal strain axes coincide

$$\theta_c = \theta \quad (17)$$

To complete the model, relationships between the principal compressive stress and the principal compressive strain and between the principal tensile stress and the principal tensile strain are required.

EXPERIMENTAL PROGRAM

To obtain the necessary information, 30 reinforced concrete elements were subjected to simple well-defined loading conditions (see Table 1). While the majority of the tests were conducted in monotonic pure shear, some elements were subjected to uniaxial compression, combined biaxial compression and shear, combined biaxial tension and shear, reversed cyclic shear, and changing load ratios. In addition to loading conditions, the prime variables included percentage of transverse reinforcement, percentage of longitudinal reinforcement, and concrete strength.

The test specimens were 890 mm square x 70 mm thick (35 x 35 x 2.75 in.). They were reinforced with two layers of welded wire mesh with the wires running parallel to the edges of the element. The smooth wire meshes typically had a 50 mm (2 in.) grid spacing, were heat-treated, and showed a ductile response. A clear cover of 6 mm (0.25 in.) was provided over the longitudinal bars. Maximum aggregate size was 6 mm (0.25 in.).

Five steel "shear keys" were cast into each of the four edges of the test specimen and were anchored to the concrete by shear studs. The specimens were loaded by forces applied to the shear keys using 37 double-acting hydraulic jacks and a network of links as shown in Fig. 7. To house the jack-and-link assembly, a steel box-section reaction frame was built (see Fig. 8). A lateral support frame was provided to resist any out-of-plane displacements of the specimens. Any combination of shear and tension or compression could be applied to the test specimens by varying the magnitude and direction of the forces in various groups of links.

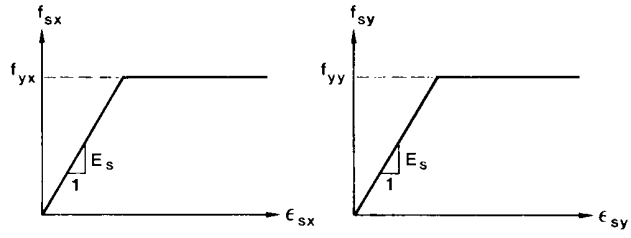

Fig. 6 — Stress-strain relationships for reinforcement

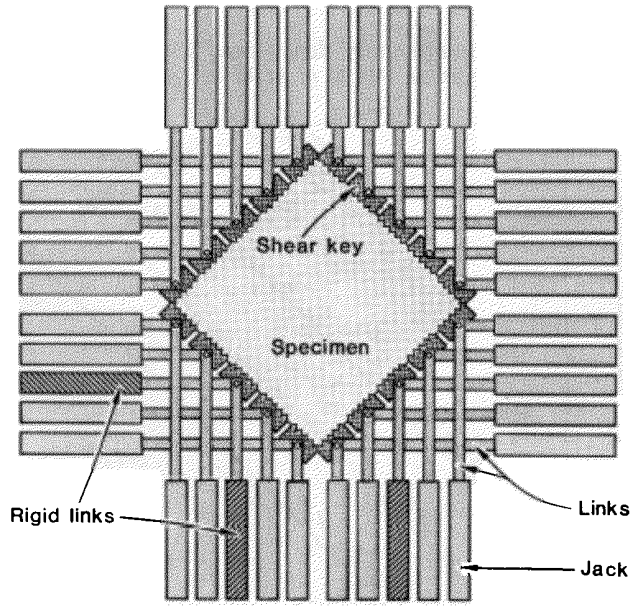

Fig. 7 — Jack-and-link assembly used to apply shear and normal stresses

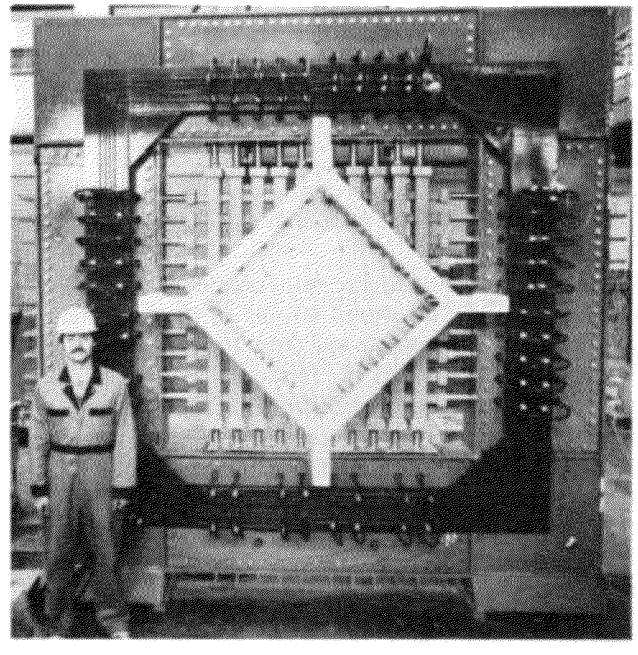

Fig. 8 — The membrane element tester

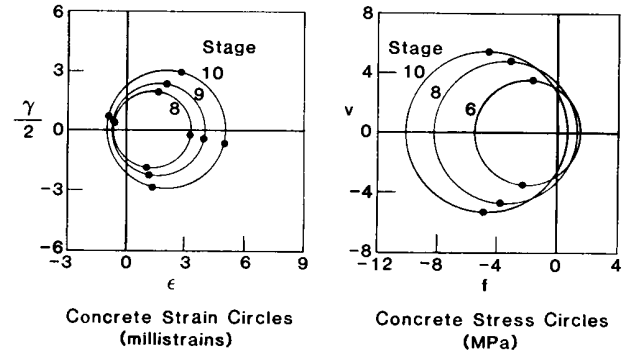

Fig. 9 — Experimentally determined strain and stress circles for Specimen PV 26 (1 MPa = 145 psi)

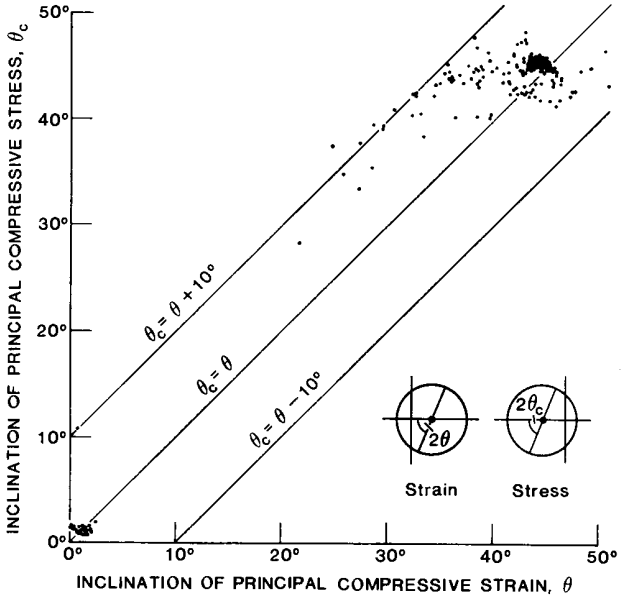

Fig. 10 — Comparison of principal compressive stress direction with principal compressive strain direction

In the tests, known values of stress were applied to the reinforced concrete (f_x, f_y, and v_{xy}), and the resulting specimen strains were measured (ϵ_x, ϵ_y, and γ_{xy}). Reference 11 gives full details of the experimental program.

Average stresses in the reinforcement were determined from the measured strains in the longitudinal and transverse directions and from the measured stress-strain characteristics of the reinforcement. Using these reinforcement stresses together with the known externally applied normal stresses, the average concrete stresses in the longitudinal and transverse directions were calculated from equilibrium Eq. (7) and (8). Knowing the applied shear stress acting on the element, the remaining concrete stress parameters could be determined. Thus, for each specimen at each load stage, it was possible to draw a concrete strain circle and a concrete stress circle (see Fig. 9). It then remained to determine relationships linking the concrete stress circles to the concrete strain circles.

AVERAGE STRESS-AVERAGE STRAIN RESPONSE OF CONCRETE

The directions of principal strains in the concrete deviated somewhat from the directions of principal stresses in the concrete (see Fig. 10). However, it remains a reasonable simplification to assume that the principal strain axes and the principal stress axes for the concrete coincide.

The principal compressive stress in the concrete f_{c2} was found to be a function not only of the principal compressive strain ϵ_2 but also of the co-existing principal tensile strain ϵ_1. Thus, cracked concrete subjected to high tensile strains in the direction normal to the compression is softer and weaker than concrete in a standard cylinder test (see Fig. 11). The relationship suggested is

$$f_{c2} = f_{c2max} \cdot \left[2\left(\frac{\epsilon_2}{\epsilon_c'}\right) - \left(\frac{\epsilon_2}{\epsilon_c'}\right)^2\right] \qquad (18a)$$

where

$$\frac{f_{c2max}}{f_c'} = \frac{1}{0.8 - 0.34\,\epsilon_1/\epsilon_c'} \leqslant 1.0 \qquad (18b)$$

Note that as ϵ_c' is a negative quantity (usually -0.002), increasing ϵ_1 will reduce f_{c2max}/f_c'.

The relationship between the average principal tensile stress in the concrete and the average principal tensile strain is nearly linear prior to cracking and then shows decreasing values of f_{c1} with increasing values of ϵ_1 (see Fig. 11). The relationship suggested prior to cracking (i.e., $\epsilon_1 \leqslant \epsilon_{cr}$) is

$$f_{c1} = E_c \cdot \epsilon_1 \qquad (19)$$

where E_c is the modulus of elasticity of the concrete which can be taken as $2f_c'/\epsilon_c'$. The relationship suggested after cracking (i.e., $\epsilon_1 > \epsilon_{cr}$) is

$$f_{c1} = \frac{f_{cr}}{1 + \sqrt{200\,\epsilon_1}} \qquad (20)$$

TRANSMITTING LOADS ACROSS CRACKS

The stress and strain formulations described deal with average values and do not give information regarding local variations. At a crack, the tensile stresses in the reinforcement will be higher than average, while midway between cracks they will be lower than average. The concrete tensile stresses, on the other hand, will be zero at a crack and higher than average midway between cracks. These local variations are important because the ultimate capacity of a biaxially stressed element may be governed by the reinforcement's ability to transmit tension across the cracks.

Fig. 12 compares the calculated average stresses (Plane 1) with the actual local stresses that occur at a crack (Plane 2). The critical crack direction is assumed normal to the principal tensile strain direction. While the calculated average shear stress on Plane 1 is zero (in

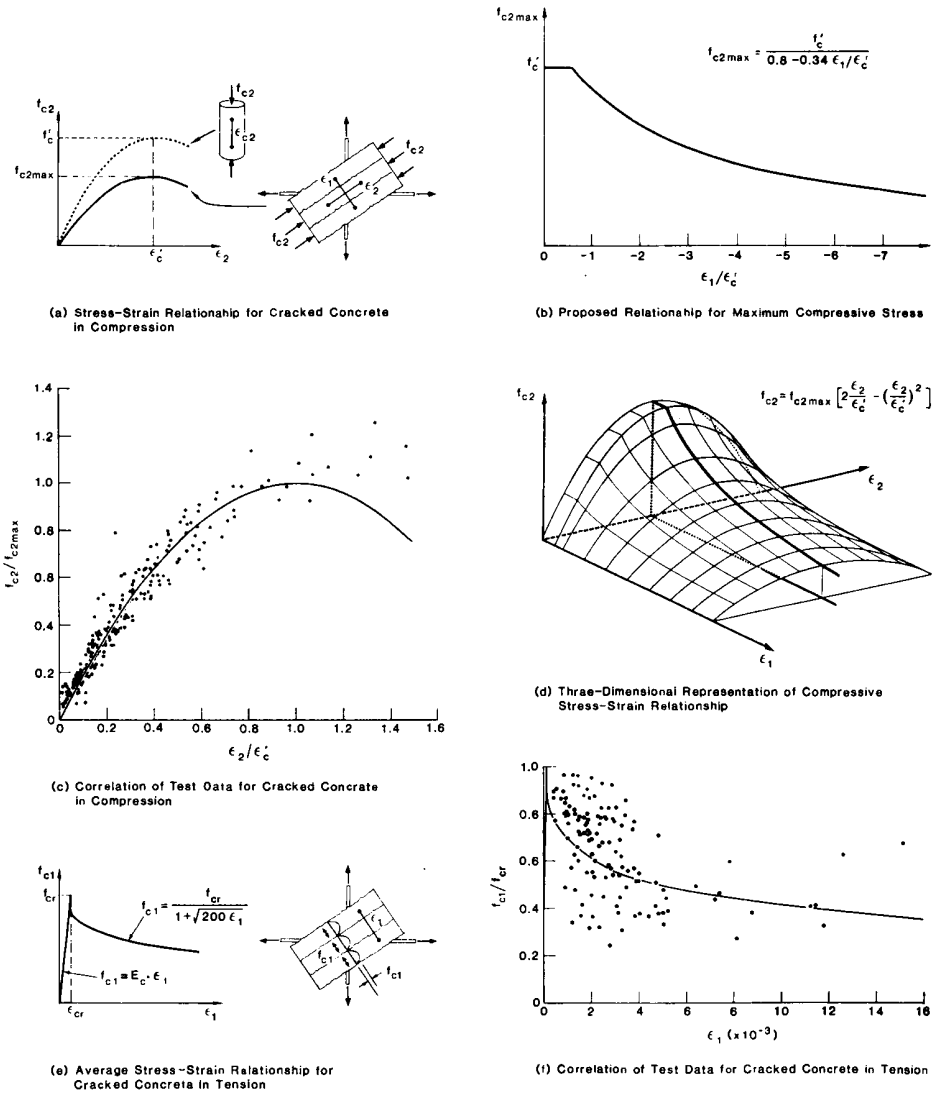

Fig. 11 — Stress-strain relationships for cracked concrete

terms of average stresses it is a principal plane), there may be local shear stresses on Plane 2. These shear stresses v_{ci}, may be accompanied by small local compressive stresses f_{ci}, across the crack.

As the applied external stresses f_x, f_y, and v_{xy} are fixed, the two sets of stresses shown in Fig. 12 must be statically equivalent. Assuming a unit area for both Plane 1 and Plane 2, the requirement that the two sets of stresses produce the same force in the x-direction is

$$\rho_{sx} f_{sx} \sin\theta + f_{ci} \sin\theta = \rho_{sx} f_{sxcr} \sin\theta - f_{ci} \sin\theta - v_{ci} \cos\theta \quad (21)$$

The requirement that the two sets of stresses on Plane 1 produce the same force in the y-direction is

$$\rho_{sy} f_{sy} \cos\theta + f_{c1} \cos\theta = \rho_{sy} f_{sycr} \cos\theta - f_{ci} \cos\theta + v_{ci} \sin\theta \quad (22)$$

Eq. (22) can be rearranged as

$$\rho_{sy}(f_{sycr} - f_{sy}) = f_{c1} + f_{ci} - v_{ci} \tan\theta \quad (23)$$

While Eq. (21) can be rearranged as

$$\rho_{sx}(f_{sxcr} - f_{sx}) = f_{c1} + f_{ci} + v_{ci}/\tan\theta \quad (24)$$

Equilibrium Eq. (23) and (24) can be satisfied with no shear stress on the crack and no compressive stresses on the crack only if

$$\rho_{sy}(f_{sycr} - f_{sy}) = \rho_{sx}(f_{sxcr} - f_{sx}) = f_{c1} \quad (25)$$

However, the stress in the reinforcement at a crack cannot exceed the yield strength, that is

$$f_{sxcr} \leqslant f_{yx} \quad (26)$$

and

$$f_{sycr} \leqslant f_{yy} \quad (27)$$

Hence, if the calculated average stress in either reinforcement is high, it may not be possible to satisfy Eq. (25). In this case, equilibrium will require shear stresses on the crack.

For the vast majority of concretes, cracking will occur along the interface between the cement paste and the aggregate particles. The resulting rough cracks can transfer shear by aggregate interlock (see Fig. 13). The relationships between the shear across the crack v_{ci}, the crack width w, and the required compressive stress on the crack f_{ci} have been experimentally studied by a number of investigators, including Walraven.[12] Based on Walraven's work, the following relationship was derived (see Fig. 14)

$$v_{ci} = 0.18\, v_{cimax} + 1.64\, f_{ci} - 0.82\, \frac{f_{ci}^2}{v_{cimax}} \qquad (28)$$

where

$$v_{cimax} = \frac{\sqrt{-f'_c}}{0.31 + 24\, w/(a + 16)} \qquad (29)$$

and where a is the maximum aggregate size in millimeters and the stresses are in MPa. If inch and psi units are being used, the numerator of Eq. (29) should be multiplied by 12, and 16 in the denominator should be replaced by 0.63.

The crack width w to be used in Eq. (29) should be the average crack width over the crack surface. It can be taken as the product of the principal tensile strain and the crack spacing s_θ; that is

$$w = \epsilon_1 \cdot s_\theta \qquad (30)$$

where

$$s_\theta = \frac{1}{\frac{\sin\theta}{s_{mx}} + \frac{\cos\theta}{s_{my}}} \qquad (31)$$

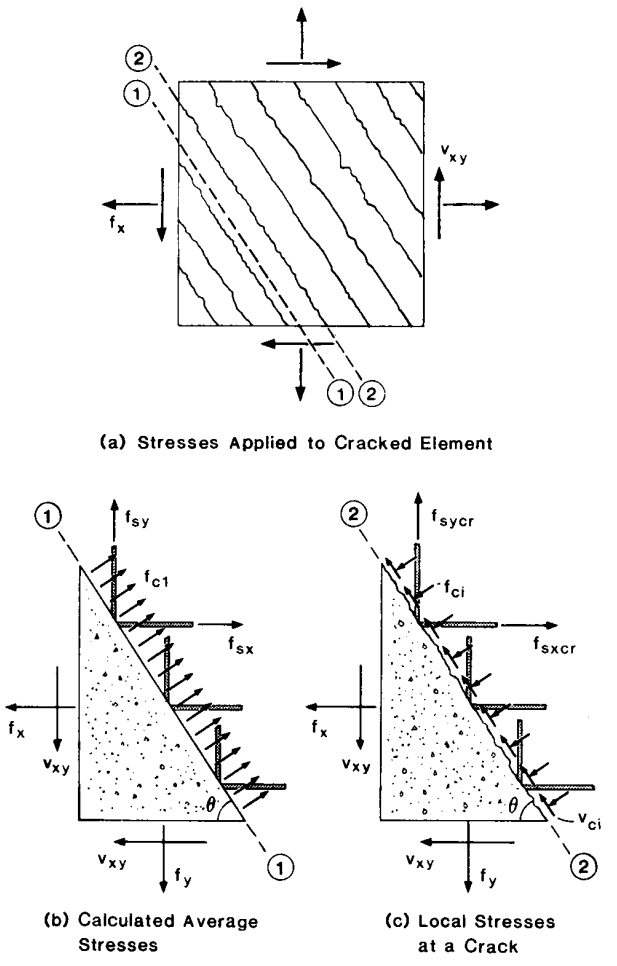

Fig. 12 — Comparison of local stresses at a crack with calculated average stresses

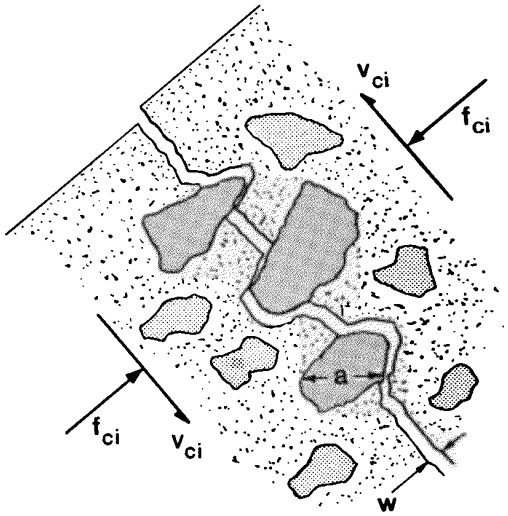

Fig. 13 — Transmitting shear stresses across crack by aggregate interlock

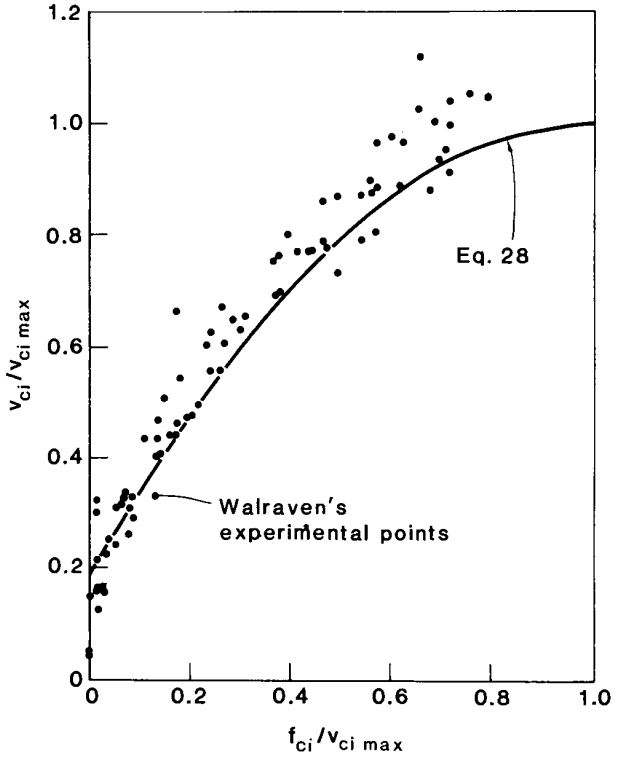

Fig. 14 — Relationship between shear transmitted across crack and compressive stress on crack

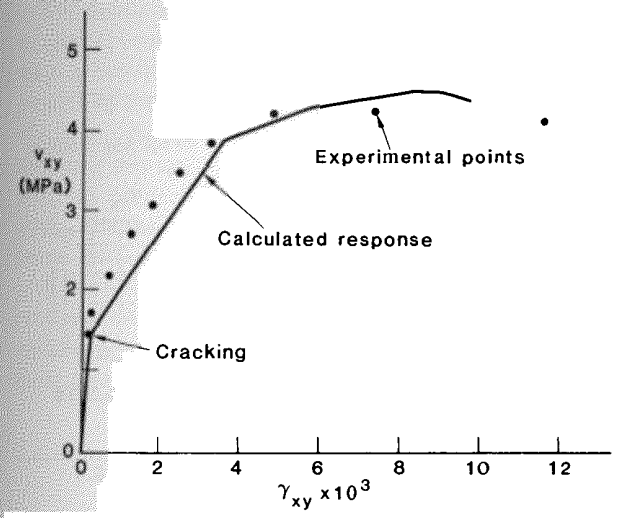

Fig. 15 — Comparison of calculated and observed response of Specimen PV20 (1 MPa = 145 psi)

and where s_{mx} and s_{my} are the indicators of the crack control characteristics of the x-reinforcement and the y-reinforcement, respectively.

Thus, in checking stress conditions at the crack surfaces, a combination of the shear and compressive stresses v_{ci} and f_{ci} must be determined to satisfy Eq. (23) through (29). If, because of steel yielding at the crack, a solution is not possible, then the calculated average principal tensile stress f_{c1} must be reduced until a solution is possible.

SOLUTION TECHNIQUE

Given the strains in a reinforced concrete element, it is a reasonably direct procedure to calculate the stresses which cause these strains. The only iteration that may be required is that involved in determining f_{ci} if the reinforcement is not capable of transmitting the tension in the concrete across the cracks.

To find the element's strains, given the stresses, is a more difficult problem that requires a trial and error solution. The Appendix presents a suitable computational procedure to determine the response of a biaxially loaded element.

EXAMPLE OF PREDICTION RESPONSE

Specimen PV20 was loaded in pure shear (see Table 1). For this specimen, the crack control parameters were estimated to be s_{mx} = 47 mm (1.9 in.) and s_{my} = 44 mm (1.7 in.), and the cracking strength of the concrete was taken to be $0.33\sqrt{-f'_c}$ = 1.47 MPa (210 psi). Using the solution procedure outlined in the Appendix, the element's response was calculated as described in Table 2 and Fig. 15. Note that at failure, the principal compressive stress in the concrete was only about 45 percent of the cylinder strength, and that even for tensile strains as high as 0.0075 the average tensile stress in the cracked concrete is predicted to be 0.66 MPa (95 psi). Fig. 16 shows the appearance of the specimen after failure. The failure can be described as a concrete shear failure.

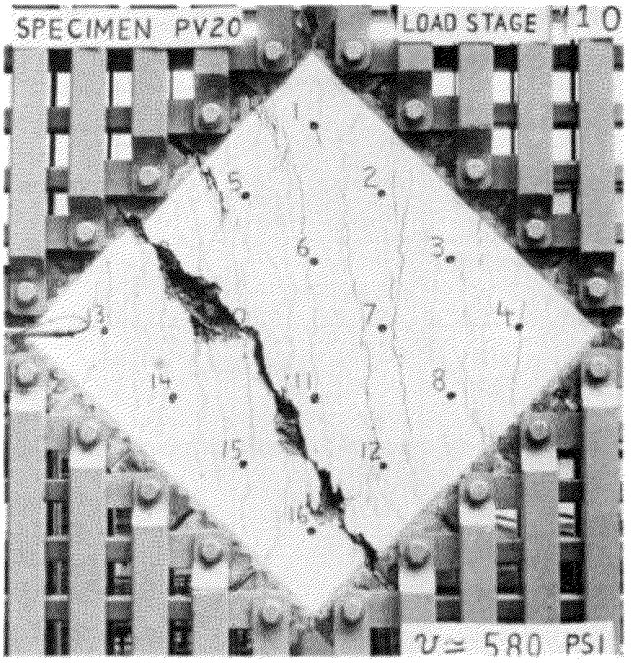

Fig. 16 — Specimen PV20 after failure

Table 2 — Predicted response of PV20

$\epsilon_1 \times 10^3$	θ_ϵ, deg	f_{cx}, MPa	f_{c1}, MPa	v_{cxy}, MPa	$\frac{f_{c2}}{f'_c}$	f_{cy}, MPa	v_{cys}, MPa	f_{sxcr}, MPa	f_{sxcr}, MPa	$\gamma_{xy} \times 10^3$	Remarks
0.067	44.9	1.6	1.31	1.33	0.06	1.5	0	147	74	0.12	Cracking
0.50	42.8	46	1.11	1.65	0.10	37	0	169	98	0.60	
1.00	42.0	97	1.01	2.11	0.16	73	0	209	129	1.15	
1.50	41.6	148	0.94	2.56	0.21	107	0	252	159	1.71	
2.00	41.4	198	0.89	3.03	0.26	140	0	296.9	189	2.29	$f_{sycr} \simeq f_{yy}$
3.00	41.3	293	0.82	3.95	0.37	203	0.90	297	305	3.50	$f_{sx} \simeq f_{yy}$
5.00	37.9	297	0.73	4.37	0.42	269	0.94	297	376	5.70	
7.00	36.3	297	0.67	4.55	0.45	305	0.91	297	410	8.06	Peak load
7.50	36.3	297	0.66	4.53	0.45	304	0.89	297	407	8.80	Concrete crushing

Note: 1 MPa = 145 psi.

SHEAR STRENGTH-AXIAL STRENGTH INTERACTION DIAGRAMS

In the test program previously described, four specimens (PV23, PV25, PV27, and PV28) with nearly identical properties were loaded at different ratios of shear stress to axial stress. In each case, $f_x = f_y$. The average material properties of the four specimens were $f'_c = -19.8$ MPa (-2870 psi) and $f_{yx} = f_{yy} = 477$ MPa (69 ksi).

Fig. 17 shows the predicted cracking loads and the predicted failure loads for elements containing 1.79 percent of both x- and y-reinforcement and having the average material properties. Also shown in Fig. 17 are the observed cracking loads and the observed failure loads for the four specimens tested.

Note that there are three rather distinct regions in the shear strength-axial strength interaction diagrams shown in Fig. 17: (1) at high biaxial tensions, yielding of the reinforcement at the cracks controls failure; (2) concrete shear failures govern in the middle regions,

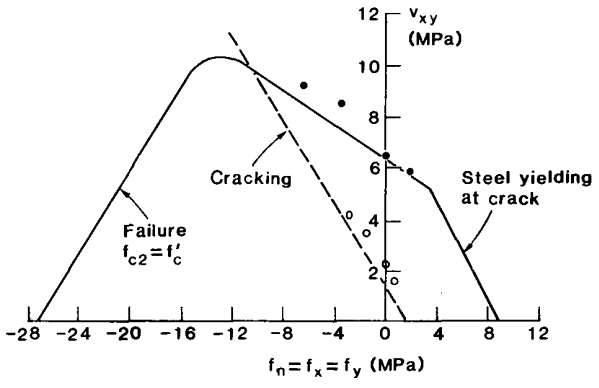

Fig. 17 — Shear strength-axial strength interaction diagram (1 MPa = 145 psi)

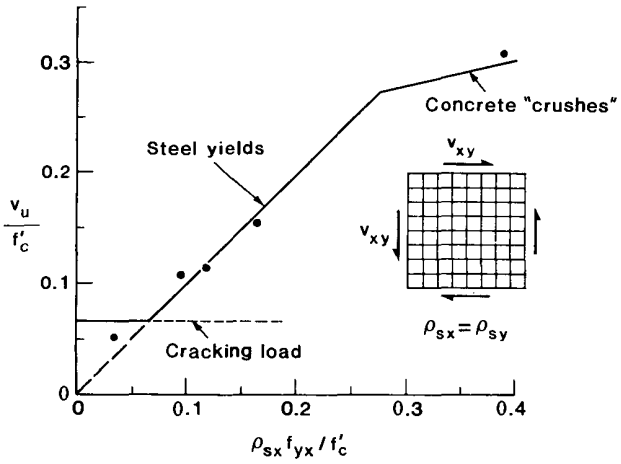

Fig. 18 — Shear strength variation as both longitudinal and transverse reinforcement are increased

with concrete failing at compressive stresses considerably less than f'_c, and (3) at high biaxial compression levels, failure is controlled by f_{c2} reaching f'_c.

INFLUENCE OF REINFORCEMENT RATIOS ON SHEAR STRENGTH

Approximately two-thirds of the specimens described in Table 1 were loaded in pure shear and had x- and y-reinforcement consisting of wires near each face at 50 mm (2 in.) centers. A study of two series of these panels will be made to learn more about how the reinforcement ratios influence shear strength.

In the first series of five tests (PV2, PV3, PV4, PV6, and PV27), the amount of transverse reinforcement was always equal to the amount of longitudinal reinforcement, but this amount varied from 0.18 to 1.79 percent. The predicted strengths were based on the following average material properties: $f'_c = -25.4$ MPa (-3680 psi) and $f_{yx} = f_{yy} = 442$ MPa (64 ksi).

Fig. 18 shows the predicted strengths together with the observed failure loads. For very small amounts of reinforcement ($\rho_{sx} < f_{cr}/f_{yx}$), the cracking load will be the maximum load which can be carried by the elements. Beyond that, for a wide range of reinforcement ratios, steel yielding will govern the failure, i.e., $v_u = \rho_{sx} \cdot f_{yx}$. For very large amounts of reinforcement, concrete shear failures will govern. Note that for these elements the ACI Code[6] approach of determining the ultimate shear capacity by adding the steel contribution to the cracking load would be unconservative.

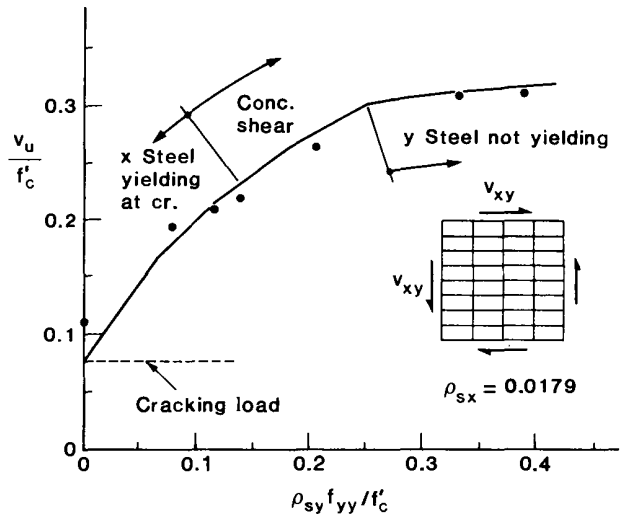

Fig. 19 — Shear strength variation as transverse reinforcement only is increased

In the second series of seven tests (PV13, PV12, PV19, PV20, PV21, PV22, and PV27), the longitudinal reinforcement was kept constant at 1.79 percent while the amount of transverse reinforcement was varied. The predicted strengths were based on the following material properties: $f'_c = -18.9$ MPa (-2740 psi) and $f_{yx} = f_{yy} = 430$ MPa (62 ksi).

Fig. 19 compares the observed and predicted ultimate shear strengths. Note that now even very small amounts of transverse reinforcement are beneficial in increasing shear strength. Yielding of the longitudinal reinforcement at the cracks limits f_{c1} and hence controls the strength for small amounts of transverse reinforcement, while concrete shear failures control the strength for larger amounts of transverse reinforcement.

CONCLUDING REMARKS

The modified compression-field theory is capable of predicting the response of reinforced concrete elements to in-plane shear and axial stresses by considering equilibrium conditions, compatibility requirements, and stress-strain relationships, all expressed in terms of average stresses and average strains. Consideration is also given to local stress conditions at crack locations. Further, newly formulated and experimentally verified constitutive relationships for cracked concrete are incorporated for principal compressive stress-principal compressive strain response, and for principal tensile stress-principal tensile strain response. The theory is schematically summarized in Fig. 20.

The modified compression-field theory is a powerful analytical tool, but is simple enough to be programmed with a handheld calculator. Not only is it capable of predicting the test results reported in this paper, but it has been used by other researchers to successfully predict their test results.[13,14] In addition, it has proved suitable for predicting the response of beams loaded in shear, flexure, and axial loads, and as a basis for nonlinear finite element analysis programs.

A large-scale test program is now underway to extend the theory to elements subjected to combined membrane stresses, bending stresses, and out-of-plane shear (see Fig. 21).

ACKNOWLEDGMENTS

The research at the University of Toronto which led to the Modified Compression Field Theory was made possible by a series of grants from the Natural Sciences and Engineering Research Council of Canada and by a grant from Ontario Hydro. The considerations of local stresses at a crack were developed by the second author while he was on research leave at the University of Canterbury. This portion of the work was funded by the Road Research Unit of the National Roads Board of New Zealand. The authors would like to express their gratitude to all three organizations for their support.

NOTATION

- a = maximum aggregate size
- E_c = modulus of elasticity of concrete (initial tangent stiffness)
- E_s = modulus of elasticity of reinforcement
- f'_c = maximum compressive stress observed in a cylinder test (negative quantity)
- f_{ct} = principal tensile stress in concrete
- f_{c2} = principal compressive stress in concrete (negative quantity)
- f_{ci} = compressive stress on crack surface (positive quantity)
- f_{cr} = stress in concrete at cracking
- f_{cx} = stress in concrete in x-direction
- f_{cy} = stress in concrete in y-direction
- f_n = normal stress applied to element
- f_{sx} = average stress in x-reinforcement
- f_{sxcr} = stress in x-reinforcement at crack location
- f_{sy} = average stress in y-reinforcement
- f_{sycr} = stress in y-reinforcement at crack location
- f_x = stress applied to element in x-direction
- f_y = stress applied to element in y-direction
- f_{yx} = yield stress of x-reinforcement
- f_{yy} = yield stress of y-reinforcement
- S_θ = spacing of cracks inclined at θ
- s_{mx} = average spacing of cracks perpendicular to the x-reinforcement
- s_{my} = average spacing of cracks perpendicular to the y-reinforcement
- v_{ci} = shear stress on crack surfaces
- v_{cimax} = maximum shear stress a crack of given width can resist
- v_{cx} = shear stress on x-face of concrete
- v_{cxy} = shear stress on concrete relative to x, y axes
- v_{cy} = shear stress on y-face of concrete
- v_{sx} = shear stress on x-reinforcement
- v_{sy} = shear stress on y-reinforcement
- v_u = maximum shear stress element can resist
- v_{xy} = shear stress on element relative to x, y axes
- w = crack width
- ϵ_1 = principal tensile strain in concrete (positive quantity)
- ϵ_2 = principal compressive strain in concrete (negative quantity)

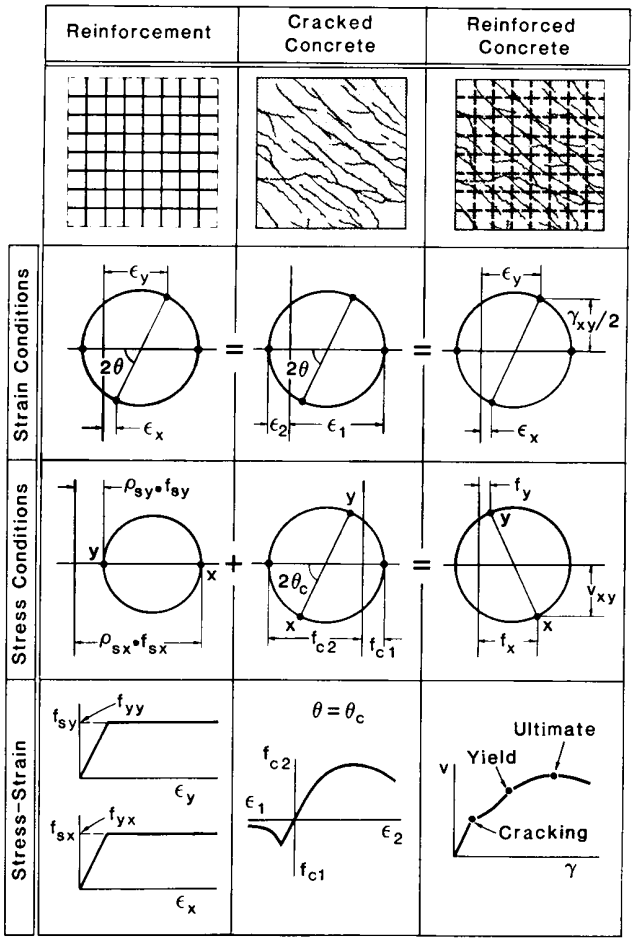

Fig. 20 — The modified compression-field theory for membrane elements

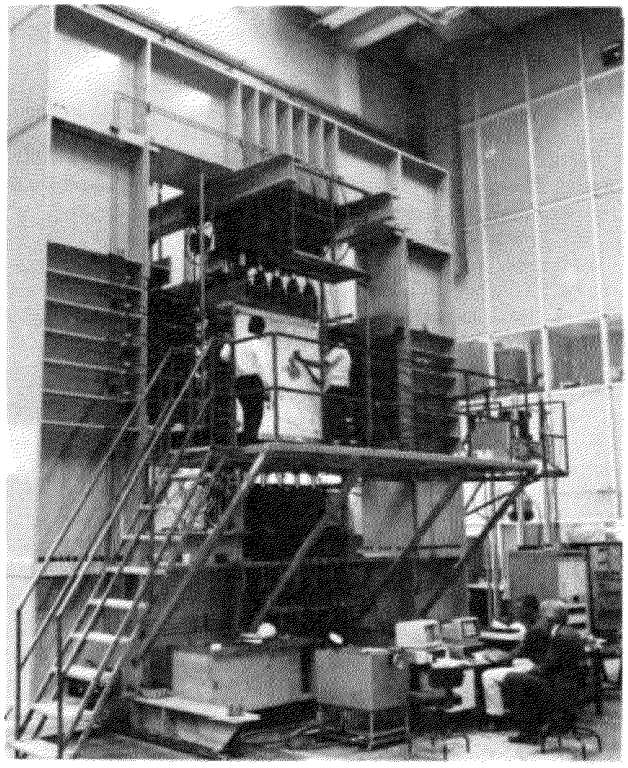

Fig. 21 — The shell element tester

ϵ_c' = strain in concrete cylinder at peak stress f_c' (negative quantity)
ϵ_{cr} = strain in concrete at cracking
ϵ_{cx} = strain in concrete in x-direction
ϵ_{cy} = strain in concrete in y-direction
ϵ_{sx} = strain in reinforcing steel in x-direction
ϵ_{sy} = strain in reinforcing steel in y-direction
ϵ_x = strain in x-direction
ϵ_y = strain in y-direction
ϵ_{yx} = yield strain of x-reinforcement
ϵ_{yy} = yield strain of y-reinforcement
γ_{xy} = shear strain relative to x, y axes
θ = angle of inclination of principal strains to x-axis
θ_c = angle of inclination of principal stresses in concrete to x-axis
ρ_{sx} = reinforcement ratio for reinforcing steel in x-direction
ρ_{sy} = reinforcement ratio for reinforcing steel in y-direction

REFERENCES

1. Zienkiewicz, O. C., *The Finite Element Method,* 3rd Edition, McGraw-Hill Book Co., New York, 1977, 787 pp.

2. Brebbia, C. A., *A Handbook of Finite Element Systems,* 2nd Edition, CML Publications, Southhampton, 1983, 500 pp.

3. Logcher, R. D., et al., "ICES STRUDL-II, The Structural Design Language, Engineering User's Manual—V. 1—Frame Analysis," *Report* No. 68-91, Department of Civil Enginering, Massachusetts Institute of Technology, Cambridge, Nov. 1968, 226 pp.

4. "Rules for Design, Construction, and Inspection of Offshore Structures, 1977, Appendix D, Concrete Structures," Det Norske Veritas, Oslo, 1980, 22 pp.

5. ACI-ASME Committee 359, "Code for Concrete Reactor Vessels and Containments," *ASME Boiler and Pressure Vessel Code,* Section III, Division 2, American Society of Mechanical Engineers, New York, 1983, 376 pp.

6. ACI Committee 318, "Building Code Requirements for Reinforced Concrete (ACI 318-83)," American Concrete Institute, Detroit, 1983, 111 pp.

7. Gupta, A. K., "Membrane Reinforcement in Concrete Shells: A Review," *Nuclear Engineering and Design,* Elsevier Science Publishers, Amsterdam, 1984, pp. 63-75.

8. Collins, M. P.; Vecchio, F. J.; and Mehlhorn, G., "An International Competition to Predict the Response of Reinforced Concrete Panels," *Canadian Journal of Civil Engineering* (Ottawa), V. 12, No. 3, Sept. 1985, pp. 626-644.

9. Mitchell, Denis, and Collins, Michael P., "Diagonal Compression Field Theory—A Rational Model for Structural Concrete in Pure Torsion," ACI JOURNAL, *Proceedings* V. 71, No. 8, Aug. 1974, pp. 396-408.

10. Collins, Michael P., "Towards a Rational Theory for RC Members in Shear," *Proceedings,* ASCE, V. 104, ST4, Apr. 1978, pp. 649-666.

11. Vecchio, F. J., and Collins, M. P., "Response of Reinforced Concrete to In-Plane Shear and Normal Stresses," *Publication* No. 82-03, Department of Civil Engineering, University of Toronto, Mar. 1982, 332 pp.

12. Walraven, Joost C., "Fundamental Analysis of Aggregate Interlock," *Proceedings,* ASCE, V. 107, ST11, Nov. 1981, pp. 2245-2270.

13. Iida, T.; Sumi, K.; and Kawamata, S., "Behavior of Orthogonally Reinforced Walls Subjected to In-Plane Shear Force—Effectiveness of F. J. Vecchio and M. P. Collins' Theory," *Proceedings,* Annual Meeting, Architectural Institute of Japan, Yokohama, Oct. 1984, pp. 1807-1809.

14. Ang, B. G., "Seismic Shear Strength of Circular Bridge Piers," PhD thesis, Department of Civil Engineering, University of Canterbury, Christchurch, 1985.

APPENDIX — SOLUTION TECHNIQUE FOR DETERMINING RESPONSE OF BIAXIALLY STRESSED ELEMENTS

It will be assumed that f_x and f_y are constant and that it is desired to find the relationship between shear stress v_{xy} and the resulting shear strain γ_{xy}. For simplicity, assume no prestressed reinforcement.

Step 1 — Determine the crack control characteristics of the x-reinforcement and the y reinforcement. Use more refined empirical equations, or s_{mx} = 1.5 × maximum distance from x-bars and s_{my} = 1.5 × maximum distance from y-bars.

Step 2 — Choose a value of ϵ_1 at which to perform the calculations.

Step 3 — Estimate principal compresssive stress direction θ.

Step 4 — Calculate average crack width w using Eq. (31) and (30).

Step 5 — Estimate average stress in weaker reinforcement; assume that this is the y-reinforcement. Hence, estimate f_{sy}.

Step 6 — Calculate average tension in the concrete f_{c1} using Eq. (19) and (20), subject to the condition that

$$f_{c1} \leqslant v_{ci max} (0.18 + 0.3k^2) \tan\theta + \rho_{sy} (f_{sy} - f_{cy})$$

where $k = 1.64 - 1/\tan\theta$, but $k \geqslant 0$; and where $v_{ci max}$ is given by Eq. (29).

Step 7 — Calculate shear stress v_{xy} from equilibrium

$$f_{cx} = f_x - \rho_{sx} f_{sx}$$

$$v_{xy} = (f_{c1} - f_{cx})/\tan\theta$$

Step 8 — Calculate f_{c2} from equilibrium using Eq. (13).

Step 9 — Calculate f_{c2max} for given ϵ_1 using Eq. (18).

Step 10 — Check that $f_{c2}/f_{c2max} \leqslant 1.0$. If greater than 1.0, then solution is not possible; return to Step 3 and choose θ closer to 45 deg or return to Step 2 and choose a lower ϵ_1.

Step 11 — Calculate ϵ_2 using Eq. (18b)

$$\epsilon_2 = \epsilon_c' \cdot (1 - \sqrt{1 - f_{c2}/f_{c2max}})$$

Step 12 — Calculate ϵ_y from geometry using Eq. (5);

$$\epsilon_y = \frac{\epsilon_1 + \epsilon_2 \cdot \tan^2\theta}{1 + \tan^2\theta}$$

Step 13 — Calculate f_{sy} using Eq. (15).

Step 14 — Check if f_{sy} calculated agrees with estimated f_{sy}. If not, return to Step 5 with new estimate of f_{sy}.

Step 15 — Calculate ϵ_x from geometry using Eq. (4).

Step 16 — Calculate f_{sx} using Eq. (14).

Step 17 — Calculate f_x from equilibrium

$$f_{cx} = f_{c1} - v_{xy}/\tan\theta$$

$$f_x = f_{cx} + \rho_{sx} f_{sx}$$

Step 18 — Check if f_x calculated agrees with given f_x. If not, return to Step 3 and make new estimate of θ. Increasing θ increases f_x.

Step 19 — Calculate stresses on crack v_{ci} and f_{ci}

$$\Delta f_{c1} = f_{c1} - \rho_{sy} (f_{sy} - f_{sy})$$

If $\Delta f_{c1} \leqslant 0$, then $v_{ci} = 0$ and $f_{ci} = 0$. Go to Step 20.

If $\Delta f_{c1} > 0$, then $C = \dfrac{\Delta f_{c1}}{tan\theta} - 0.18\, v_{c1max}$

If $C \leqslant 0$, then $f_{c2} = 0$ and $v_{c2} = \Delta f_{c1}/tan\theta$

Otherwise

$$A = 0.82/v_{c1max} \text{ and } B = \frac{1}{tan\theta} - 1.64$$

$$f_{c2} = (-b - \sqrt{B^2 - 4AC})/2A$$

$$v_{c2} = (f_{c1} + \Delta f_{c1})/\tan\theta$$

Step 20 — Calculate reinforcement stresses at crack f_{syer} and f_{sxer}

$$f_{syer} = f_{sy} + (f_{c1} + f_{c2} - v_{c2}tan\theta)/\rho_{sy}$$

$$f_{sxer} = f_{sx} + (f_{c2} + f_{c1} + v_{c2}/tan\theta)/\rho_{sx}$$

Step 21 — Check that reinforcement can carry stresses at crack. Because of the way in which v_{c2} and f_{c2} were calculated, f_{syer} will not exceed f_{sy}. However, the calculated value of f_{sxer} may exceed f_{sx}. If it does, the reinforcement is not capable of transmitting the loads across the crack; assume a lower f_{c2} and return to Step 7.

Step 22 — Calculate shear strain γ_{xy} from geometry

$$\gamma_{xy} = 2\,(\epsilon_1 - \epsilon_2)/tan\theta$$

To obtain the complete response of the element, these calculations are repeated for a range of values of ϵ_1, starting from ϵ_1 less than cracking ($\epsilon_1 \simeq 0.05 \times 10^{-3}$) and increasing ϵ_1 until the maximum shear is obtained.

If at failure:

i. f_{c1} is limited by the condition in Step 6, then slipping on the crack governs the failure.

ii. f_{c2} is limited by f_{c2max}, then crushing or shear failure of the concrete governs.

iii. f_{c1} is limited by the requirement that $f_{sxer} \leqslant f_{sx}$, then yielding of the *x*-reinforcement at the crack governs.